

Record high temperature, high output power red VCSELs

Klein Johnson, Mary Hibbs-Brenner, William Hogan, Matthew Dummer, Kabir Dogubo, Garrett Berg, Vixar, 15350 25th Ave N, Suite 110, Plymouth, MN 55447 USA

ABSTRACT

Red VCSELs are of interest for medical and industrial sensing, printing, scanning, and consumer electronics applications. This paper will describe the optimization of red VCSEL design to achieve improved output power and a broader temperature range of operation. We will also discuss alternative packaging approaches and in particular will describe non-hermetic packages and performance of the VCSELs in a humid environment.

Record output power of 14mW CW and a record maximum temperature of operation of 105°C have been achieved at an emission wavelength of 680nm. The achievement is the result of attention to many details including resonance cavity-gain peak offset, material choices, current and mode confinement approaches, and metal aperture design. We have also demonstrated lifetimes >1000 hours for non-hermetic packages in an 85% humidity environment. A chip on board approach has been used to create a large scale linear array of VCSELs for a scanning application.

Keywords: VCSEL, Red VCSEL, red laser, 670nm

1. INTRODUCTION

Multi-mode 850nm VCSELs based upon the AlGaAs materials system have been the standard optical source for application to glass fiber optic based data communication links. However, the implementation of VCSELs for other applications frequently requires different wavelengths and performance attributes than those the 850nm multi-mode VCSELs have been optimized for.

As a first example, a very important optically based non-invasive medical sensor application is oximetry. Pulse oximetry is well-established, and tissue or regional oximetry is an emerging application. Both versions of oximetry take advantage of the varying absorption coefficient as a function of wavelength for different types of hemoglobins, i.e. oxyhemoglobin, reduced hemoglobin, carboxyhemoglobin, or methemoglobin. The sensors rely on the absorption of wavelengths in the regime from about 660nm to 1000nm, and as the number of components one wishes to distinguish increases, the number of different wavelengths that one needs to employ also increases. These applications benefit from the narrow spectral linewidth and the slow spectral shift with temperature of the VCSEL, while wireless implementations benefit from the reduced power consumption of VCSELs as compared to LEDs. However, wavelengths spanning the range from red to near-infrared are required, and in particular, the red wavelength is an important component of these systems.

A second example application is plastic fiber links based upon PMMA fiber materials which have been implemented for sensor and data links in automobiles, and are being considered for home networks. PMMA-based fiber has a primary absorption minima in the green, and a secondary absorption minima in the red. Absorption at 850nm is too high for all links more than a few meters. While the potential for high speed data rates and the packaging simplicity of VCSELs makes them ideal for this application, wavelengths in the range of 650-680nm are a necessity for low loss links. However, since these fiber links are intended for the consumer market, a low cost non-hermetic package is a necessity.

Other applications, such as printing or bar code scanning, require single spatial mode devices. Achievable print resolution is improved by the use of shorter laser wavelengths, and a beam visible to the eye is much preferred for bar code scanners.

Vixar has been developing a laser scanner with no moving parts for computed radiography, a form of x-ray imaging that results in a digitized image by storing the x-ray image in a storage phosphor screen, and then reading out the phosphor with a red laser. The red laser stimulates the emission of blue light which is detected and digitized. However, the width

of the standard screen, 14 inches, requires a fairly long optical path for scanning with a single laser. A linear laser array could reduce the size of the scanning mechanism, and make the equipment more robust. This application requires a wavelength in the 650-700nm range. However, creating a linear array of lasers 14 inches long requires tiling array chips in a chip on board configuration, again placing new requirements for packaging for this application.

Red VCSELs based upon the AlGaAs/AlGaInP materials system were first demonstrated in the early 1990's but have taken significantly longer to commercialize. Part of this is due to materials issues, such as the limited confinement potentials for quantum well structures, the small available contrast in refractive index available in the AlGaAs mirrors due to the need to use compositions that are not absorbing at 650-700nm, and the higher thermal resistance in the mirrors also resulting from the more limited composition range in the mirrors.

A second issue limiting commercialization is the requirement of many non-data communication applications for alternative packaging options. While the packaging flexibility is a strength of VCSEL technology, it often comes with additional challenges. Traditionally, the 850nm data communication VCSEL products are packaged in a hermetic TO style package. On the other hand, a disposable medical sensor may require a plastic surface mount package that incorporates an organic encapsulant, raising questions of humidity resistance. Similarly the plastic optical fiber applications will likely require low-cost non-hermetic packaging. The laser scanner design described above necessitated development of an approach for tiling array chips directly on the board in a manner that maintains VCSEL to VCSEL pitch across chip boundaries. These packaging approaches are technology development efforts that must be carried out in parallel with the basic chip development.

This paper will describe the improvements that have been achieved that now make red VCSELs practical for implementation in these new applications.

2. BACKGROUND

The earliest reports of red VCSEL demonstrations were from Sandia National Labs and Chiao Tung University in Taiwan.^{1,2,3} Some of this work was initially based upon the use of InGaAlP materials for both the quantum well active region and the mirrors, but fairly quickly most researchers adopted a structure that retained the InGaAlP based quantum well active region, but used AlGaAs materials in the mirrors, all on a GaAs substrate, thus simplifying the challenge of growing lattice-matched structures. The initial devices were limited in output power and temperature range, as might be expected from the earliest demonstrations of a new technology.

Since the early 1990's when the initial red VCSEL research was done, several groups have reported performance improvements. Calvert, et al⁴ reported the continuous wave operation of 670nm single mode devices to a heat sink temperature of 80C, while Knigge et al⁵ has demonstrated 650nm VCSELs achieving output powers of 4.3mW at room temperature, with lasing to 65°C, and 10mW at 670nm (room temperature) with lasing to 86°C. Johnson and Hibbs-Brenner reported an output power of 11.5mW at 673nm at room temperature.⁶ Sale et al⁷ has also demonstrated CW lasing at 666nm to 80°C. Additionally, a 20°C output power of 0.6mW at 650nm has been demonstrated at the Tyndall National Institute.⁸ Duggan et al⁹ have reported upon the performance and reliability of red VCSELs developed for fiber optic applications, demonstrating a 3dB bandwidth of >3 GHz and 1.25 Gbps large signal modulation. They also present data indicating lifetimes in the hundreds of thousands of hours at low currents.

Several groups have reported efforts to extend the VCSEL wavelength into the range from 700-740nm.^{10,11,12,13,14,15} All of these efforts have been based upon the AlGaAs materials system for both the mirrors and the active regions. The performance has been limited in output power and maximum temperature of operation. In some cases^{13,14,15} the device only operated in pulsed mode at room temperature, while in other results^{10,11,12} the devices did operate CW at room temperature, but the output power was limited to less than 1mW.

The goals of the work reported here are to increase the output power, temperature range of operation, achievable wavelength range, and reliability of VCSELs in the red wavelength region. Specifically, we have targeted a minimum of 1mW single mode power from 0-60°C, 10mW multi-mode power up to 40°C, and at least 1mW of useable multi-mode power at 80°C. Our goal is also to extend performance to 720nm with > 1mW of useable output power.

3. APPROACH

The red VCSEL structure is illustrated schematically in Figure 1. The structure is grown on 4" n+-GaAs substrates. Mirrors are AlGaAs based with graded interfaces between the high and low index layers. The active region consists of strained InGaP quantum wells with an AlGaInP barriers and confining region. A highly doped contact layer is grown at the top surface to facilitate formation of ohmic contacts.

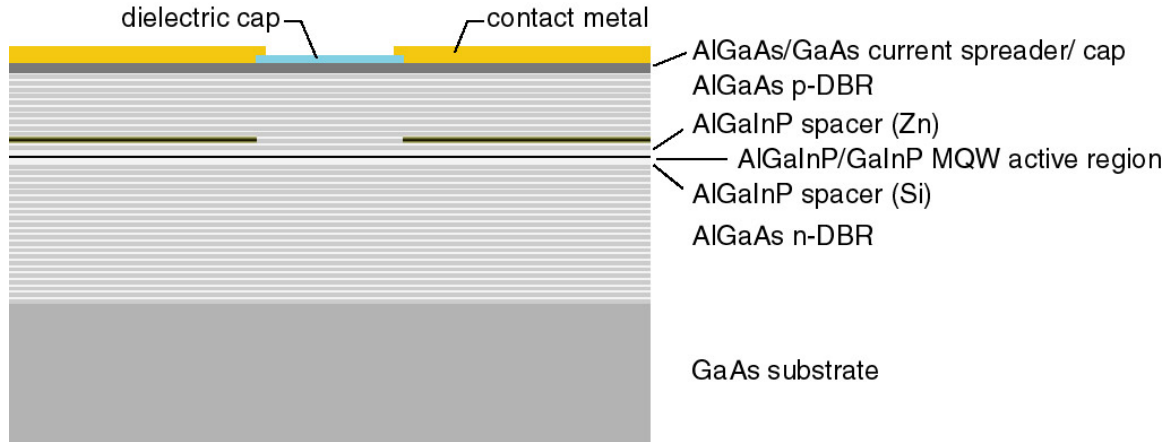


Figure 1. Schematic of VCSEL structure.

Current and index confinement is provided by an oxide confinement layer. The devices are top-emitting, with a broad-area gold contact made to the back side of the device, and a ring contact patterned around the current aperture on the front side of the device. A variety of aperture sizes were included on the mask to evaluate performance as a function of aperture size. Some die consisted of an array of apertures connected to a common anode in order to increase the total power output that could be achieved.

Wafers were probed on an automated probe station with a temperature controlled chuck. 100% probe testing of the light output and voltage versus drive current (L-I-V) and wavelength was performed at 40°C. L-I-V measurements were made over a range of temperatures on a sample basis. Devices were packaged in a TO-46 header for measurement of beam profiles, and for measurement of pulsed characteristics.

Reliability measurements under pulsed conditions were carried out on devices in hermetic TO-46 packages. Resistance to humidity was evaluated at 50°C, 85% humidity on devices packaged in TO-46 headers but with the glass window removed from the lid. In both cases devices are biased during life testing at the accelerated environmental conditions. However, the devices are removed from the oven at each test point, and tested at room temperature and humidity, which was typically 20-25°C and 40% relative humidity.

4. RESULTS

4.1 Temperature performance

One of the most challenging aspects of designing red VCSELs has been achieving useable output power over the temperature ranges required by the various applications. Figure 2 illustrates the temperature performance of two 680nm devices: a single-mode design, and a multi-mode design. The single mode device (Figure 2(a)) lases up to 115°C, with 1mW of output power achievable at 75°C, and 0.5mW at 95°C. We believe that this is the highest temperature operation achieved in red VCSELs. Generally, the temperature range of operation of larger diameter, multi-mode devices is more limited. Figure 2(b) illustrates the temperature performance of a multi-mode 680nm VCSEL. This device ceases to lase somewhere between 90 and 100°C, but produces 1.5 mW of power at 80°C.

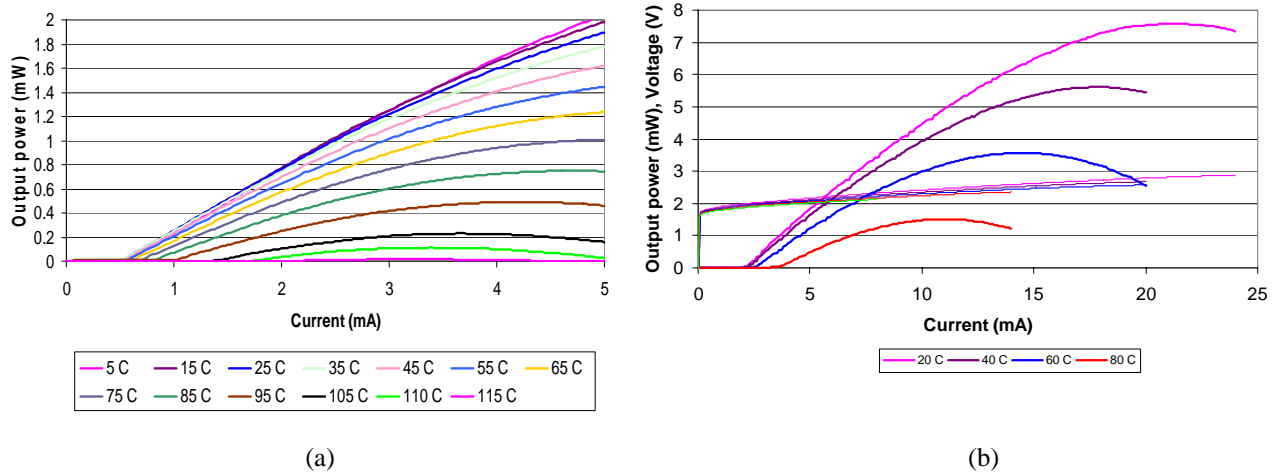


Figure 2. Light output and voltage versus current (L-I-V) at a range of temperatures for (a) a single-mode device, and (b) a multi-mode device

4.2 Single-mode performance

Figure 3 further illustrates the performance of single-mode devices. Figure 3(a) overlays the L-I-V curves of an array of single-mode VCSELs. Figure 3(b) shows the beam profile of one of the devices in the array. Profiles in the x- and y-direction are taken at three different currents, i.e. 4, 5 and 6mA and are overlaid in the figure of intensity versus angle. It is difficult to distinguish more than one plot since the three plots overlap so closely. Single spatial mode performance is maintained up to the current corresponding to the peak output power.

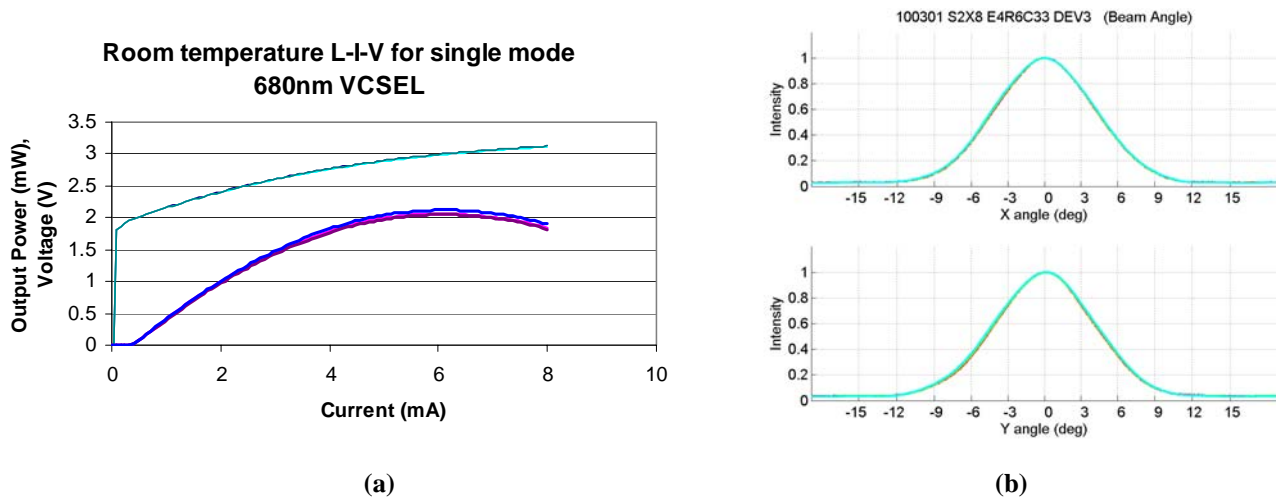


Figure 3. Performance of single-mode VCSELs. (a) Overlaid L-I-V curves from a 1x3 array. (b) Beam intensity versus angle in the x- and y- direction at three current levels: 4,5, and 6mA.

4.3 Wafer uniformity: wavelength and device performance

One of the key questions of interest in the production of devices is the uniformity across a wafer. The wavelength of a VCSEL is approximately proportional to thickness of the layers, so a 1% variation of thickness can result in approximately a 7nm variation in wavelength. In addition, the oxidation diameter can also vary across a wafer due to small differences in layer thickness, doping or composition. Both of these effects can impact performance of a VCSEL. For instance, the temperature characteristics of a VCSEL depend upon the offset between the gain peak and the Fabry-

Perot resonance. Since the gain peak wavelength is less sensitive to thickness and therefore nearly constant across the wafer, while the Fabry-Perot resonance may have a range of 5-10nm, this offset varies across the wafer. The ability to do automated wafer scale testing allows us to gather statistics on uniformity.

Figure 4 shows the results of probing approximately 60,000 VCSELs on a 4" wafer. A histogram of the wavelength distribution of the devices is shown in Figure 4(a). While the distribution ranges from 675nm to 709nm, the vast majority of the devices on the wafer lie in the range from 681 to 689nm. Figure 4(b) illustrates the uniformity of threshold current as a function of emission wavelength for four different laser aperture sizes. This data (and the data in Figure 4(c) was taken at 40°C. The shaded region in the figure corresponds to the wavelength range constituting the majority of the devices on the wafer. Threshold currents are less than 0.5mA for the smallest devices and around 2.5 to 3mA for the 15µm apertures at 40°C. While the largest diameter devices appear to be quite a bit less uniform than the smallest diameter, on a percentage basis the threshold current range of the 15µm device is similar to that of the 7 and 10µm devices. As one might expect, the threshold current rises as the emission wavelength increases, due to a larger offset between the gain peak and the Fabry-Perot cavity, but devices are still lasing at 709nm, where the offset is approximately 40nm. Peak output power at 40°C versus wavelength for several aperture sizes is shown in Figure 4(c). Note that the 15µm aperture device power is shown as negative. This was our code for indicating that the output power had not yet reached a peak at the maximum current tested, and hence underestimates the peak output power. Within the wavelength region included in the shaded region, which includes the majority of the VCSELs on the wafer, the peak output power is quite uniform.

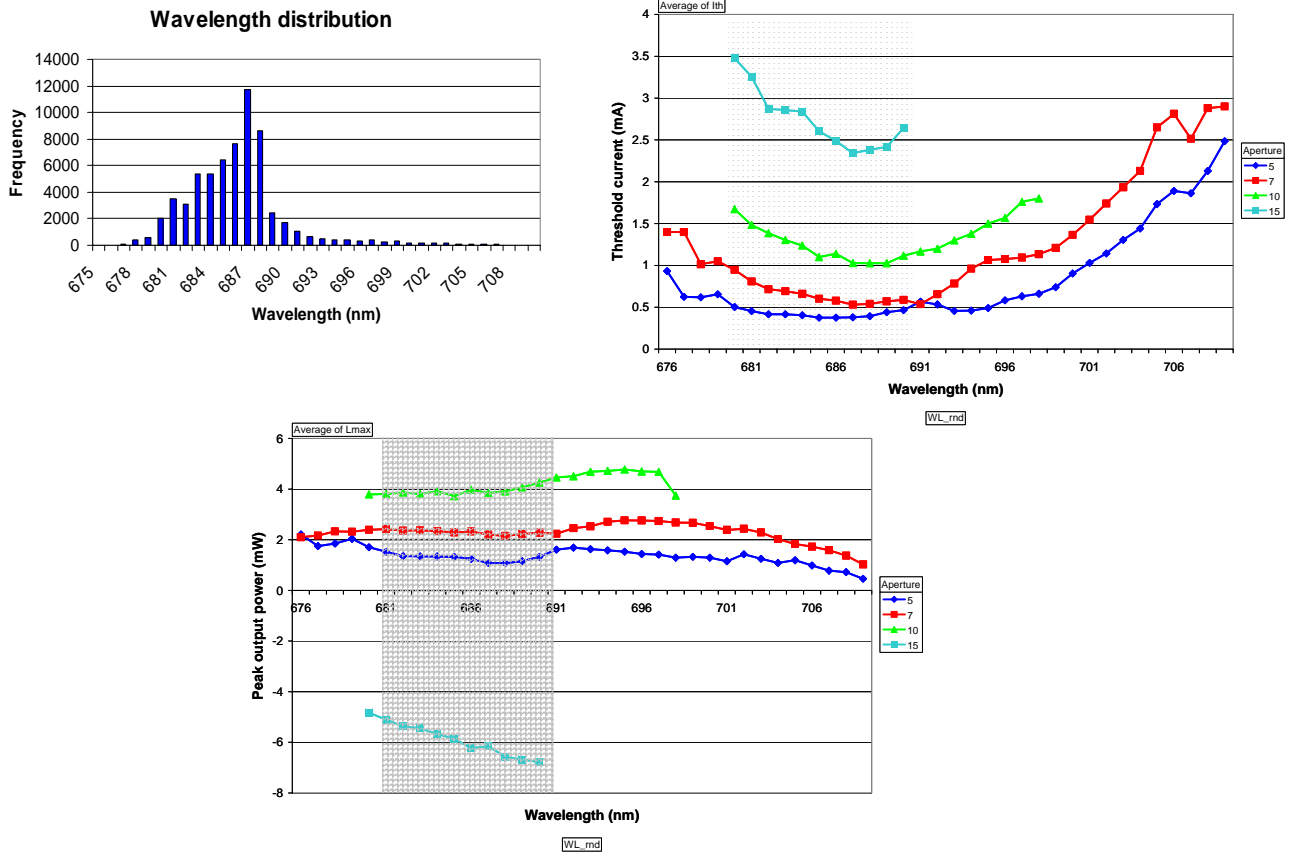


Figure 4. (a) Histogram showing the wavelength distribution of 60,000 VCSELs tested at 40°C on a 4" wafer. (b) Threshold current versus wavelength. (c) Peak output power versus wavelength. Negative numbers for output power indicate that the peak output power was not reached within the drive current test range, and so underestimates peak output power. The shaded regions in 4(b) and 4(c) indicate the wavelength range corresponding to the vast majority of devices on the wafer.

4.4 Maximum achievable output power

Red VCSELs have typically been limited in the maximum output power that can be achieved from a conventional all-epitaxial structure, in part because the larger aperture devices are more sensitive to temperature. Improved thermal design has allowed larger devices to be built. Figure 5 illustrates the output power achievable from two types of devices. Figure 5(a) shows the L-I-V from a single, large diameter aperture device. The device emits a peak output power of 14mW. If beam size or optical quality are not an issue, an alternative way of achieving high output power is to use multiple apertures with a common anode contact. Figure 5(b) illustrates that nearly 45mW of output power at room temperature can be generated from an array of apertures within a 200 μ m x 200 μ m area.

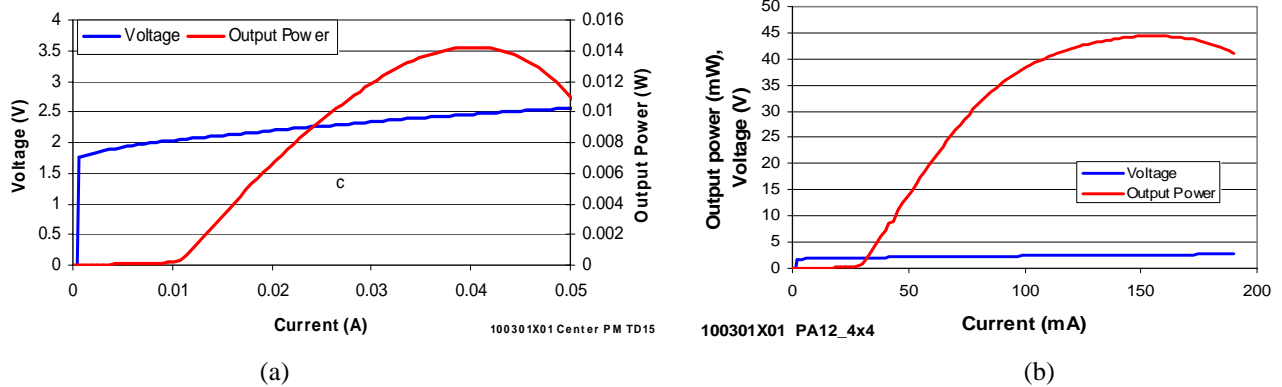


Figure 5. High output power devices. (a) L-I-V curve from a device with a single large aperture, demonstrating a peak output power of 14mW. (b) L-I-V from a device with multiple apertures in a 200 μ m x 200 μ m area, demonstrating a peak output power of 44mW.

4.5 Extended wavelength performance

We have fabricated devices with wavelengths in the range from 700-720nm, but unlike previous reports, our devices are based upon GaInP/AlGaInP active regions. A large variation in wavelength across a single wafer was achieved by not rotating the wafer during growth. The gain peak wavelength was fairly constant at around 678nm, while the Fabry-Perot resonance varied from 680 up to nearly 720nm. The longest wavelengths, therefore, corresponded to a very large gain peak-Fabry Perot resonance offset, as large as 40nm. Figure 6 shows the results from two devices at the higher end of the wavelength range. The devices lased CW at room temperature. A 716nm device (Figure 6(a)) had a threshold current of 7mA and a peak output power of nearly 3.5mW, while a 718.8nm device had a threshold current of 7mA and a peak output power of over 2mW. The threshold current is high due to the large gain peak-resonance offset, so it is believed that even better performance could be achieved if the devices were optimally designed for this wavelength. We therefore believe that good VCSEL performance spanning the entire wavelength range from 650 to 850nm can be achieved using either the AlGaAs materials system, or the AlGaInP materials for the active region.

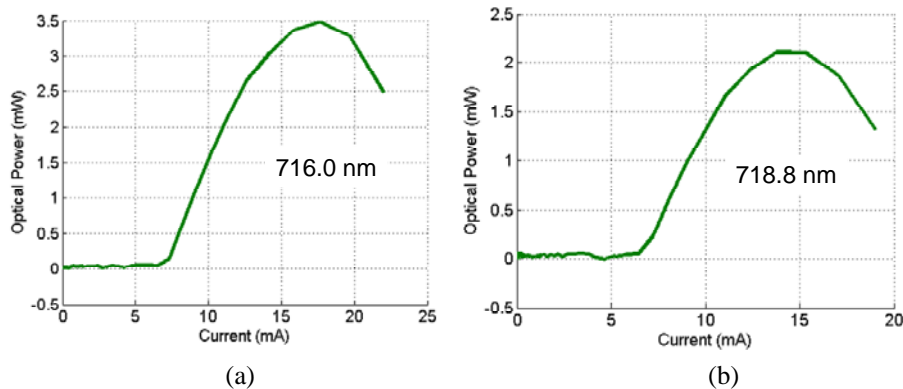


Figure 6. Performance of an AlGaInP QW based VCSEL in an extended wavelength regime. (a) 716.0nm, and (b) at 718.8nm.

4.6 Pulsed operation and reliability.

There are some applications where lasers are typically pulsed at a low duty cycle, such as industrial sensors, or the computed radiography application described in the introduction. The pulse width could be in the range of 1 μ sec, while the duty cycle might be less than 25%. It has been demonstrated at other wavelengths that the peak output power can be extended significantly due to the reduction in self-heating when pulsed. Red VCSELs are even more limited by thermal effects and hence we desired to quantify the magnitude of potential improvement that could be achieved if the devices were pulsed.

Figure 7 illustrates the performance of a multi-mode 680nm VCSEL operated in pulsed mode. The relevant parameters affecting pulsed performance are pulse width, duty cycle and ambient temperature. Since 1 μ sec is a nominal thermal time constant for a VCSEL chip, pulse widths substantially longer than this provide little benefit. We have used 1 μ sec pulse width for the evaluation, although shorter pulse widths can provide even higher peak power. Figure 7(a) illustrates the effect of the duty cycle on improved peak output power. A 10% duty cycle can provide nearly a 4X improvement in peak power, while a 50% duty cycle still provides nearly a 2X increase in peak power. Also note that the peak power achieved at a 10% duty cycle exceeds 35mW. This is a multi-mode device with a single aperture. Figure 7(b) illustrates the improvement in the temperature range of operation that can be achieved when the device is pulsed at a 25% duty cycle. The peak power of the device at 60°C reaches 15mW, while under CW operation, the same device might only reach a peak power of 3-4mW.

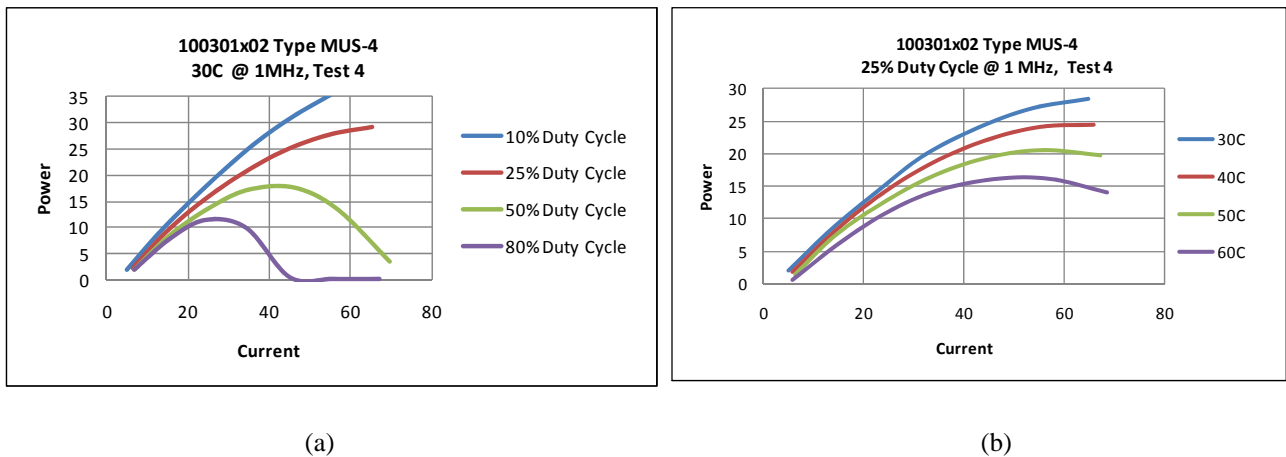


Figure 7. Output power versus current for multi-mode 680nm VCSELs operated in pulsed mode with a 1 μ sec pulse width. (a) illustrates the effect of varying the duty cycle, while (b) illustrates the improved temperature performance associated with pulsed operation.

As mentioned, in pulsed mode the device self-heating is reduced, and therefore the device rollover point (where increasing the current actually results in a reduction of output power) is extended to significantly higher drive current. However, this leads to a question: if device lifetime is reduced by higher current drives, can one operate a device in pulsed mode at these higher current ranges without impacting the device lifetime? Furthermore, are there any transient effects, such as stress created by repeated temperature cycling resulting from the current cycling, that might actually accelerate the degradation of the devices? For instance, the dependence of VCSEL lifetime upon current density is commonly found to be reduced proportionally to the square of the current density, i.e. a 2X increase in current density would reduce device lifetime by a factor of 4. An increase of drive current from 15mA to 60mA might be expected to reduce the lifetime by a factor of 16.

Therefore, we developed a capability for testing the VCSELs in pulsed mode. Both single-mode and multi-mode devices were packaged in TO-46 headers and mounted on boards that were placed in ovens. The devices were pulsed with a pulse width of 1 μ sec, and a duty cycle of 12.5%. Thus 8 hours of test time correspond to 1 hour of actual “on-time” The devices were periodically removed from the oven and tested CW at room temperature, and then returned to the oven for further aging under pulsed conditions. The results are illustrated in Figure 8.

Pulsed reliability test, 670nm VCSELs

50 C, Pulse width 1usec, 12.5% duty cycle

7mA (single-mode)

18 and 30mA (multi-mode)

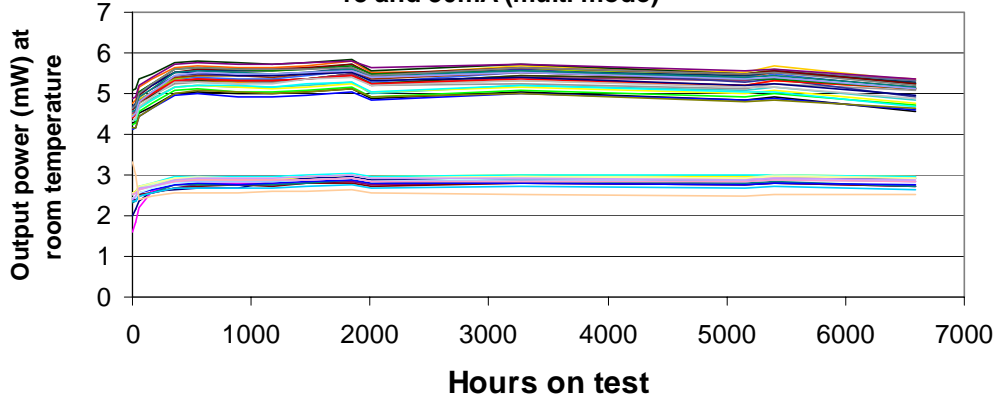


Figure 8. Peak output power versus test time for devices tested in pulsed mode. The output power testing was performed at room temperature. The lower curves correspond to a smaller diameter single-mode device, while the upper curves correspond to a multi-mode device.

The multi-mode devices have an output power around 5mW and were pulsed to one of two different current levels, 18mA or 30mA. The single-mode devices have an output power of approximately 2.5 to 3mW and were pulsed to 7mA. A burn-in effect can be seen in the first 100-200 hours, where the output power increases, but after the burn-in period, the output power has been stable during the 6596 hours of test at 50°C, corresponding to 824 hours of actual pulsed on-time.

Table 1 illustrates the differences in acceleration factor one might expect for the CW and pulsed cases. In this table we compare acceleration factors based on the assumption of a use condition at 25°C, and 10mA. We have measured the thermal resistance of the multimode device, and found it to be 1.4°C/mW. We assume acceleration factors which have been reported in reference [9] for red VCSELs, i.e. an Arrhenius relationship for temperature dependence with an activation energy of 0.6eV, and a squared dependence on current. These acceleration factors are also representative of that routinely reported for 850nm VCSELs. We also assumed a thermal resistance of 0 in the pulsed case.

Table 1. Calculation of acceleration factors assuming a use condition of 10mA and 25°C.

DC or pulsed	Current	Acceleration factor
DC	10	4.5
	18	88
	30	2438
pulsed	10	6
	18	20
	30	55

While we do not yet have sufficient data to project a lifetime, this table predicts a very significant improvement in lifetime under pulsed conditions, assuming no transient effects, which is consistent with our observations. We would certainly expect devices operated CW at 30mA at 50°C for the equivalent of 824 hours to have failed. The table above indicates that 824 hours at 50°C and 30mA would be equivalent to more than 2 million hours at the use conditions of 25°C and 10mA. We also cannot completely rule out acceleration due to thermal transients when operated under pulsed conditions, but the lack of degradation observed in Figure 8 suggests that this is not a significant consideration. During 6596 test hours, at a period of 8μsec, the devices have experienced approximately 3 trillion pulses.

4.7 Non-hermetic packaging and humidity effects.

In order to address some applications that are non-conventional uses of VCSELs, Vixar is developing packaging approaches that are non-hermetic. Two are illustrated in Figure 9. Figure 9(a) shows a low cost surface mount package, a PLCC-4, or plastic leaded chip carrier with 4 leads, which uses a clear organic encapsulant rather than a lid. The package accommodates up to 3 independently modulated chips, allowing for multiple colors in the same 3mm x 3mm package, for instance. It is shown in Figure 9 with two chips. Figure 9(b) illustrates array of VCSELs for a scanning application, implementing a chip on board approach. The array contains sixteen 1x32 array chips for a total of 512 lasers on a 100 μ m pitch.

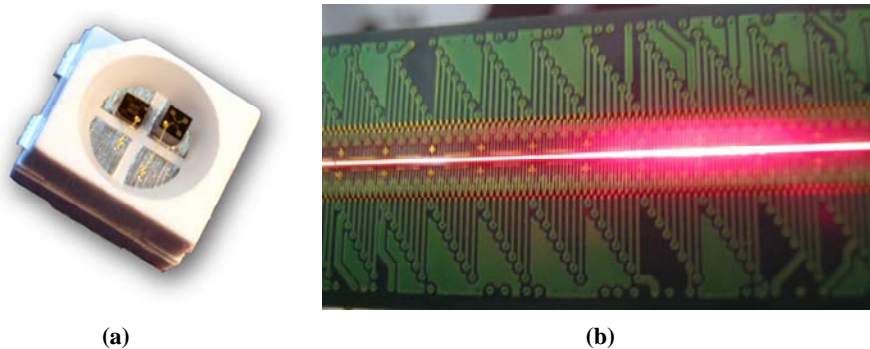


Figure 9. (a) A PLCC-4 package incorporating 2 VCSEL chips. The package dimensions are 2.8mm x 3.2mm. (b) Sixteen 1 x 32 VCSEL arrays implemented in a chip on board (COB) approach.

However, most active optical devices are sensitive to a humid environment, and VCSELs are no exception. Therefore we have performed environmental testing on our chips under accelerated conditions of temperature and humidity. Thirty chips were packaged in a TO can with the window removed and placed on boards in a chamber held at 50°C and 85% humidity. Five came from a wafer designed to improve humidity resistance, were placed in non-hermetic packages and were powered during the test (Fig. 10, upper left) with 5mA of drive current. As controls we included three other categories of devices. Five parts from a wafer without the enhancement for humidity resistance were packaged in hermetic packages and powered with 5mA of drive current (Fig. 10 upper right), fifteen parts from three different wafers without the design improvement for humidity resistance were placed in non-hermetic packages and powered with 5mA (Fig. 10, lower left) and five parts without the design for humidity resistance were packaged in non-hermetic packages but not powered during test (Fig. 10, lower right).

The parts were periodically removed from the environmental chamber, and tested at room temperature and approximately 30-40% humidity. The performance is summarized in Figure 10. After 1473 hours, all five devices with the design enhancement, non-hermetic packaging, and powered during test are still demonstrating stable output power. However, 14 out of the 15 devices from three different wafers without the design enhancement, in non-hermetic packages and powered during test have failed by 500 hours. Five devices from one of the same wafers without the design enhancement for humidity resistance, but not powered during life-testing, are all still stable after 1473 hours. Devices without the design enhancement, but packaged in a hermetic package are still stable at 1473 hours. The conclusions from this study are that humidity combined with current drive dramatically accelerates the failure of VCSELs without the design enhancement, but that the design enhancement significantly improves humidity resistance.

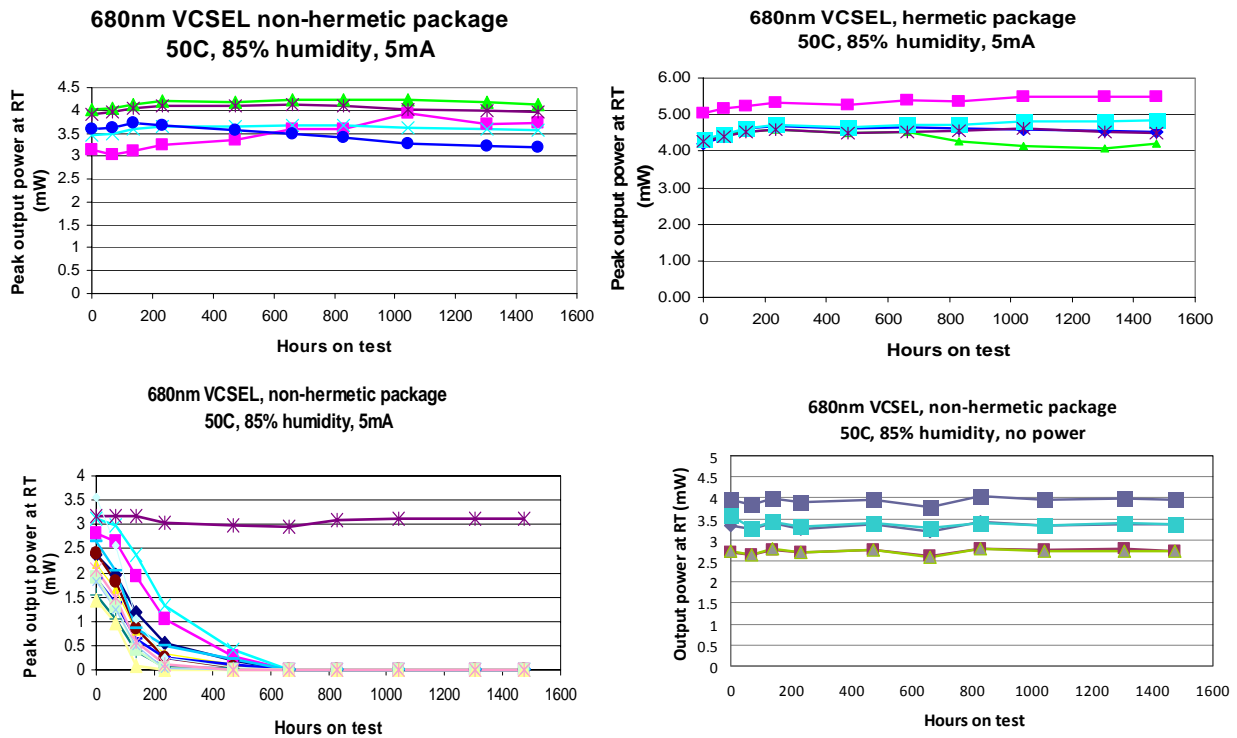


Figure 10. Output power versus hours on accelerated life testing for 680nm VCSELs. Devices were maintained at 50°C and 85% humidity during the test, but were periodically removed and L-I-V measurements were made at room temperature and humidity. Upper left: Devices from a wafer with changes designed to improve humidity resistance, in non-hermetic packaging, held at 5mA during test. Upper right: Devices from a wafer without the enhancements for humidity resistance, in a hermetic packaging and powered during test. Lower left: devices from 3 different wafers without improvements for humidity resistance, non-hermetic packaging, and powered at 5mA during the test. Lower right: Devices without improvement for humidity resistance, in non-hermetic packaging, but not powered during the test.

5. SUMMARY AND CONCLUSIONS

The results reported in this paper describe substantial improvements in the temperature range of operation, the magnitude of output power and the range of wavelengths that can be achieved in red VCSELs. The improved performance is the result of attention to many details of the design including quantum well active layer design, mirror design, mask layout, proper choice of gain peak resonance cavity offset, and epitaxial materials quality. There is no silver bullet, but the improvement is the result of the accumulation of many incremental steps of optimization.

We have demonstrated red VCSELs lasing up to 115°C for smaller aperture single mode devices and to nearly 100°C for multi-mode VCSELs. Of more importance is the temperature range of “useable” power. Single mode devices have produced 1mW of output power up to 60°C, and multi-mode devices provide up to 1.5mW of power at 80°C. We have also achieved 14mW of output power at room temperature from a single VCSEL aperture, and as much as 44mW of power from a chip containing multiple apertures within a small area.

We have been able to extend the range of wavelengths achievable from this materials system out to 719nm, with 2mW of output power at room temperature at that wavelength. While VCSELs in this wavelength range have been demonstrated in the AlGaAs materials system, our results exceed the output power achieved by the previously reported results.

We have also investigated the benefits of pulsing the VCSEL which is a useful mode of operation for some applications. Peak output power from one multi-mode aperture in excess of 35mW has been demonstrated for a 10% duty cycle and 1µsec pulse width. Pulsing also allows us to extend the temperature range of operation of the VCSELs. Concerns about potential additional acceleration of failure due to repeated thermal transitions have been allayed by reliability data showing stable operation out to nearly 6500 hours when pulsed at 30mA and a 12.5% duty cycle.

Vixar has demonstrated large scale production capability with a 4" wafer diameter process, and automated wafer probe testing that allows us to gather statistics on uniformity. Wavelength uniformity across the wafer is approximately 8nm, and average threshold current and output power uniformity do not vary significantly within that wavelength range.

The feasibility of using low cost non-hermetic packages was demonstrated by 1473 hours of continuous operation at 50°C and 85% humidity in a package open to the environment.

Red VCSEL technology has struggled to reach the marketplace due to the limitations caused by the greater materials challenges in overcoming thermal and environmental demands. We believe that the results reported here illustrate devices that are ready for use in a wide variety of applications.

ACKNOWLEDGEMENTS

This material is based upon work supported by the National Science Foundation under Grant No. IIP-0823022. Any opinions, findings, and conclusions or recommendations expressed in this material are those of the author(s) and do not necessarily reflect the views of the National Science Foundation.

REFERENCES

- [1] Lott, J.A. and Schneider, R.P., "Electrically-injected visible (639-661nm) vertical cavity surface emitting lasers," *Electronics Letters* 29, 830-832 (1993).
- [2] Huang, K.F., Tai, K., Wu, C.C., Wynn, J.D., "Continuous wave visible InGaP/InGaAlP quantum well surface emitting laser diodes," *LEOS'93 Conference Proceedings IEEE*, 613 (1993).
- [3] Chow, W.W., Choquette, K.D., Crawford, M.H., Lear, K.L. and Hadley, G.R., "Design, fabrication, and performance of infrared and visible Vertical-Cavity Surface-Emitting Lasers," *IEEE J. Quant Elect* 33(10), 1810-1823 (1997).
- [4] Calvert, T., Corbett, B. and J.D. Lambkin, "80C continuous wave operation of an AlGaInP based visible VCSEL", *Electron. Lett.* 83, 222-223 (2002).
- [5] Knigge, A., Zorn, M., Weyers, M. and Trankle, G., "High-performance vertical-cavity surface-emitting lasers with emission wavelength between 650 and 670nm", *Electron. Lett.* 38, 882-883 (2002).
- [6] Johnson, K. and Hibbs-Brenner, M.K., "High output power 670nm VCSELs" *Proc SPIE* 6484, 648404 (2007).
- [7] Sale, T.E., Knowles, G.C., Sweeney, S.J., Onischenko, A., Frost, J.E.F., Pinches, S.M. and Woodhead, J., "-180 to +80.C CW lasing in visible VCSELs", *Proceedings of IEEE LEOS Annual Meeting*, MB5 (2000).
- [8] <http://www.tyndall.ie/PDFs/vscel.pdf>
- [9] Duggan, G., Barrow, D.A., Calvert, T., Maute, M., Huang, V., McGarvey, B., Lambkin, J.D. and T. Wipiejewski, "Red Vertical Cavity Surface Emitting Lasers (VCSELs) for consumer applications", in *Vertical-Cavity Surface-Emitting Lasers XII*, *Proc. SPIE* 6908, 6908-14 (2008).

- [10] Hou, H.Q., Choquette, K.D., Hammons, B.E., Breiland, W.G., Crawford, M.H., and Lear, K.L., "Highly uniform and reproducible visible to near-infrared vertical-cavity surface-emitting lasers grown by MOVPE", Proc. SPIE 3003, 34-45 (1997).
- [11] Hou, H.Q., Crawford, M.H., Hammons, B.E., and Hickman, R.J., "Metalorganic vapor phase epitaxial growth of all-AlGaAs visible (700nm) vertical-cavity surface-emitting lasers on misoriented substrates", Journal of Electronic Materials 26, 1140-1144 (1997).
- [12] Rinaldi, F., Ostermann, J.M., Kroner, A., and Michalzik, R., "High performance AlGaAs-based VCSELs emitting in the 760nm wavelength range", Optics Communications 270, 310-313 (2007).
- [13] Sale, T., Roberts, J., Woodhead, J., David, J., and Robson, P., "Room temperature visible (683-713 nm) all-AlGaAs vertical-cavity surface-emitting lasers (VCSELs)", IEEE Photonics Technology Letters 8, 473-475, (1996).
- [14] Tell, B., Leibenguth, R., Brown-Goebeler, K., and Livescu, G., "Short wavelength (699nm) electrically pumped vertical-cavity surface-emitting lasers", IEEE Photonics Technology Letters 4, 1195-1196 (1992).
- [15] Tell, B., Brown-Goebeler, K., and Leibenguth, R., "Low temperature continuous operation of vertical-cavity surface-emitting lasers with wavelength below 700nm", IEEE Photonics Technology Letters 5, 637-639 (1993).